# Experimental and Theoretical Studies on Constitutional Isomers of 2,6-Dihydroxynaphthalene Carbaldehydes. Effects of Resonance-Assisted Hydrogen Bonding on the Electronic Absorption Spectra

Hirohiko Houjou,* Takatoshi Motoyama, Seisaku Banno, Isao Yoshikawa, and Koji Araki

Institute of Industrial Science, University of Tokyo, 4-6-1 Komaba, Meguro-ku, Tokyo 153-8505, Japan

houjou@iis.u-tokyo.ac.jp
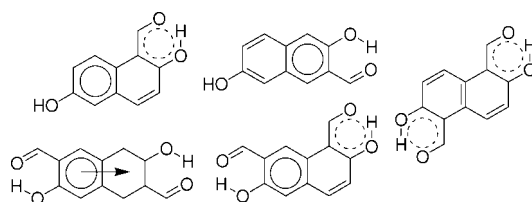
We prepared and characterized a series of mono- and dicarbaldehydes of 2,6-dihydroxynaphthalene that bear potential resonance-assisted hydrogen bonding (RAHB) unit(s). X-ray crystal structures of selected compounds revealed that each salicylaldehyde moiety forms an intramolecular hydrogen bond and that the introduction of formyl groups into either the α- or β-position causes a considerable difference in geometry, which was interpretative from a conventional scheme of resonance hybrids including ionic state. Analyses on NMR chemical shifts suggested that the compounds in solution are present as an equilibrium mixture between closed and open forms with respect to RAHB units. Ab initio calculations indicated that the formation of an intramolecular hydrogen bond strikingly influences the aromaticity of the individual local six-membered ring of naphthalene. The trend of the change in aromaticity was analyzed in connection with the extra stabilization energy of RAHB. In the UV−vis spectra, the β-formyl derivatives specifically showed a substantial red shift compared to α-formyl derivatives. The absorption features were successfully reproduced by TD-DFT calculation, and those data were consistently explained from the effects of RAHB on electronic state of the naphthalene's π-system. Finally, we pointed out a similarity in the electronic state between RAHB-bearing molecules and cata-condensed aromatic hydrocarbons.

Introduction

Dihydroxynaphthalenes, by virtue of their π-electron-rich character, are often employed as electron-donor components in supramolecular systems and as antioxidants or radical scavengers in drug and therapeutic research areas.[1−8] Among these compounds' possible constitutional isomers, 2,6-dihydroxynaphthalene attracts considerable interest because it can be oxidized to amphi-naphthoquinone, a compound in which aromaticity is lost due to drastic reconfiguration of the π system. However, the physical and chemical characteristics of *amphi*-naphthoquinone have not been researched as thoroughly as have those of *o*- and *p*-naphthoquinones.[9−13]

(1) Kim, H.-J.; Heo, J.; Jeon, W. S.; Lee, e.; Kim, J.; Sakamoto, S.; Yamaguchi, K.; Kim, K. *Angew. Chem.* **2001**, *113*, 1574–1577. Jeon, W. S.; Kim, E.; Ko, Y. H.; Hwang, I.; Lee, J. W.; Kim, S.-Y.; Kim, H.-J.; Kim, K. *Angew. Chem., Int. Ed. Engl.* **2005**, *44*, 87–91. Lee, J. W.; Kim, K.; Choi, S. W.; Ko, Y. H.; Sakamoto, S.; Yamaguchi, K.; Kim, K. *Chem. Commun.* **2002**, 2692–2693.
(2) Ballardini, R.; Balzani, V.; Gandolfi, M. T.; Gillard, R. E.; Stoddart, J. F.; Tabellini, E. *Chem.—Eur. J.* **1998**, *4*, 449–459.
(3) Mukhopadhyay, P.; Iwashita, Y.; Shirakawa, M.; Kawano, S.; Fujita, N.; Shinkai, S. *Angew. Chem., Int. Ed.* **2006**, *45*, 1592–1595.
(4) Dax, C.; Duffieux, F.; Chabot, N.; Coincon, M.; Sygusch, J.; Michels, P. A. M.; Blonski, C. *J. Med. Chem.* **2006**, *49*, 1499–1502.
(5) Bilger, C.; Demerseman, P.; Buisson, J.-P.; Royer, R.; Gayral, P.; Fourniat, J. *Eur. J. Med. Chem.* **1987**, *22*, 213–219.

(6) Sörgel, S.; Azap, C.; Reissig, H.-U. *Eur. J. Org. Chem.* **2006**, 4405–4418.
(7) Przybylski, P.; Małuszyńska, M.; Brzezinski, B. *J. Mol. Struct.* **2005**, *750*, 152–157.
(8) Sashidhara, K. V.; Rosaiah, J. N.; Nzrendar, T. *Tetrahedron Lett.* **2007**, *48*, 16991702;Sashidhara, K. V.; Rosaiah, J. N. *Tetrahedron Lett.* **2007**, *48*, 3285–3287.
(9) Adams, R.; Wankel, R. A. *J. Am. Chem. Soc.* **1951**, *73*, 2219–2220.
(10) Sugiura, K.; Saika, M.; Sakata, Y. *Chem. Lett.* **1999**, *83*, 3–834.
(11) Manimala, M.; Horak, V. *J. Electrochem. Soc.* **1986**, *198*, 7–1988.
(12) Stiborová, M.; Schmeiser, H. H.; Frei, E. *Cancer Lett.* **1999**, *146*, 53–60.

As prepared, 2,6-dihydroxynaphthalene is redox-active, and the introduction of a formyl functionality ortho to the hydroxyl group yields a unique subgroup of double-headed salicylaldehyde analogues that are extensively studied because they can be used to create a variety of macrocyclic and polymeric Schiff bases and their associated transition-metal complexes.[14−22] For salicylaldehyde and related compounds, the ground state is described as a resonance hybrid of the phenol−aldehyde (covalent) state and the protonated quinoid−enolate (ionic) state.[23] For this character of the ground state, the intramolecular hydrogen bond suffers enhanced stabilization by electronic delocalization along a proton-bridged quasi-six-membered ring and, hence, is perceived as resonance-assisted hydrogen bonding (RAHB),[24,25] although its coverage is still controversial.[26] For salicylaldehydes, RAHB is also relevant to intramolecular proton transfer in the excited state.[27−29] An RAHB unit affects the electronic state of its neighboring aromatic rings, on which an electronic "push and pull" effect of the substituents operates. When such compounds serve as a ligand in a metal complex system, the electronic state of the metal may be allowed to couple with that of the ligand's π-electron system, affording such interesting phenomena as valence tautomerism.[30−32] Previously, dioximato complexes of copper and nickel were prepared from 2,6-dihydroxynaphthalene-1,5-dicarbaldehyde (**3**), and these compounds exhibit semiconducting performance for
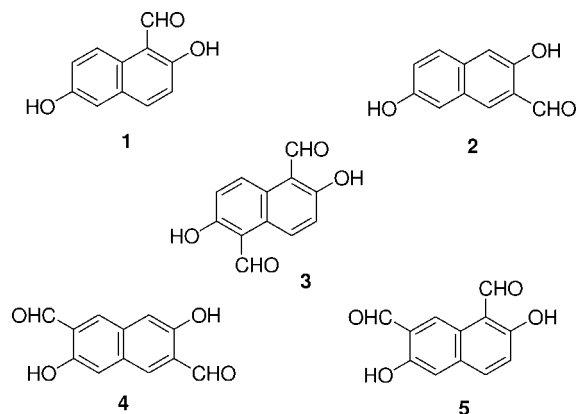
FIGURE 1. 2,6-Dihydroxynaphthalene carbaldehydes investigated in this study.

SCHEME 1. Formylation of 2,6-Dihydroxynaphthalene[a]

1 (42%) + **2** (7%)

+ {**3**+**4**, nonseparated} (20%)   +

+ **4** (10%)

6 (3%)
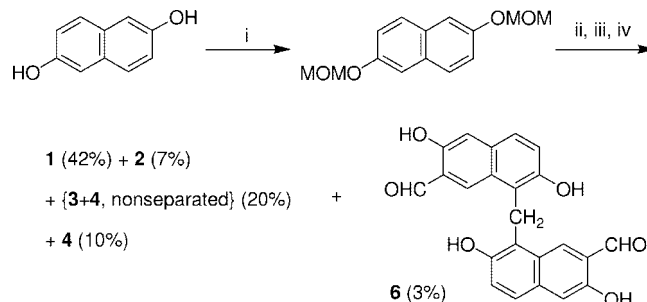
[a] Key: (i) NaH, chloromethyl methyl ether/DMF (0 °C); (ii) *n*-butyllithium/hexane−THF (−20 °C); (iii) DMF (25 °C); (iv) HCl/EtOH (80 °C).

electronic functional materials applications.[33] Despite such promising results, overall the literature contains surprisingly few studies using **3** and other related analogues of 2,6-dihydroxynaphthalene (Figure 1). This lack of comprehensive characterization data may be partly attributed to difficulties associated with the synthesis of these compounds, such as poor regioselectivity of substitution.

We herein report the structural and spectroscopic studies of the mono- and diformyl derivatives of 2,6-dihydroxynaphthalene carbaldehydes. We have synthesized **1**−**4** out of those listed in Figure 1, and the experimental data are analyzed by means of ab initio quantum chemical calculations to elucidate the effects of RAHB units on the electronic state of naphthalene ring. This study will provide insight into the electronic structure of their derivatives, allowing their optimization for use in the development of new drugs and materials.

Results and Discussion

Synthesis of Mono- and Dicarbaldehydes. The hydroxyl groups of 2,6-dihydroxynaphthalene were protected with a methoxymethyl group, and the compound was double-metalated with *n*-butyllithium and then treated with dimethylformamide and deprotected with hydrochloric acid (Scheme 1).[34,35] This reaction yielded a mixture of 2,6-dihydroxynaphthalene-1-carbaldehyde (**1**), 3,7-dihydroxynaphthalene-2-carbaldehyde (**2**),

(13) Nakatsuji, K.; Sugiura, K.; Kitagawa, T.; Toyoda, J.; Okamoto, H.; Okaniwa, K.; Mitani, T.; Yamamoto, H.; Murata, I.; Kawamoto, A.; Tanaka, J. *J. Am. Chem. Soc.* **1991**, *113*, 1862−1864. Tamura, K.; Kato, Y.; Ishikawa, A.; Kato, Y.; Himori, M.; Yoshida, M.; Takashima, Y.; Suzuki, T.; Kawabe, Y.; Cynshi, O.; Kodama, T. *J. Med. Chem.* **2003**, *46*, 3083−3093.
(14) Borisova, N. E.; Reshetova, M. D.; Ustynyuk, Y. A. *Chem. Rev.* **2007**, *107*, 46−79.
(15) Leung, A. C.; MacLachlan, M. J. *J. Inorg. Organomet. Polym. Mater.* **2007**, *17*, 57−89.
(16) Houjou, H.; Lee, S.-K.; Hishikawa, Y.; Nagawa, Y.; Hiratani, K. *Chem. Commun* **2000**, *219*, 7−2198. Houjou, H.; Tsuzuki, S.; Nagawa, Y.; Hiratani, K. *Bull. Chem. Soc. Jpn.* **2002**, *75*, 831−839. Houjou, H.; Sasaki, T.; Shimizu, Y.; Koshizaki, N.; Kanesato, M. *Adv. Mater.* **2005**, *17*, 606−610. Houjou, H.; Shimizu, Y.; Koshizaki, N.; Kanesato, M. *Adv. Mater.* **2003**, *15*, 1458−1461.
(17) Akine, S.; Hashimoto, D.; Saiki, T.; Nabeshima, T. *Tetrahedron Lett.* **2004**, *45*, 4225−4227. Nabeshima, T.; Miyazaki, H.; Iwasaki, A.; Akine, S.; Saiki, T.; Ikeda, C. *Tetrahedron* **2007**, *63*, 3328−3333.
(18) Asato, E.; Chinen, M.; Yoshino, A.; Sakata, Y.; Sugiura, K. *Chem. Lett.* **2000**, *67*, 8−679.
(19) Shimakoshi, H.; Takemoto, H.; Aritome, I.; Hisaeda, Y. *Tetrahedron Lett.* **2002**, *43*, 4809−4812.
(20) Nomura, R.; So, Y.; Izumi, A.; Nishihara, Y.; Yoshino, K.; Masuda, T. *Chem. Lett.* **2001**, *91*, 6−917.
(21) Hui, J. K.-H.; MacLachlan, M. J. *Chem. Commun.* **2006**, 2480−2482. Gallant, A. J.; Hui, J. K.-H.; Zahariev, F. E.; Wang, Y. A.; MacLachlan, M. J. *J. Org. Chem.* **2005**, *70*, 7936−7946. Gallant, A.; Yun, M.; Sauer, M.; Yeung, C. S.; MacLachlan, M. J. *Org. Lett.* **2005**, *7*, 4827−4830.
(22) Dai, Y.; Katz, T. J. *J. Org. Chem.* **1997**, *62*, 1274−1285. Dai, Y.; Katz, T. J.; Nicholas, D. A. *Angew. Chem., Int. Ed. Engl.* **1996**, *35*, 2109−2111.
(23) Borisenko, K. B.; Bock, C. W.; Hargittai, I. *J. Phys. Chem.* **1996**, *100*, 7426−7434.
(24) Gilli, G.; Bellucci, F.; Ferretti, V.; Bertolasi, V. *J. Am. Chem. Soc.* **1989**, *111*, 1023−1028.
(25) Sobczyk, L.; Grabowski, S. J.; Krygowski, T. M. *Chem. Rev.* **2005**, *105*, 3513−3560.
(26) Sanz, P.; Mó, O.; Yáñez, M.; Elguero, J. *ChemPhysChem* **2007**, *8*, 1950−1958. Sanz, P.; Mó, O.; Yáñez, M.; Elguero, J. *J. Phys. Chem. A* **2007**, *111*, 3585−3591. Sanz, P.; Mó, O.; Yáñez, M.; Elguero, J. *Chem.−Eur. J.* **2008**, *14*, 4225−4232.
(27) Palusiak, M.; Simon, S.; Sola, M. *Chem. Phys.* **2007**, *342*, 43−54.
(28) Cuma, M.; Scheiner, S.; Kar, T. *J. Am. Chem. Soc.* **1998**, *120*, 10497−10503. Cuma, M.; Scheiner, S.; Kar, T. *THEOCHEM* **1999**, *467*, 37−49.
(29) De, S. P.; Ash, S.; Dalai, S.; Misra, A. *THEOCHEM* **2007**, *807*, 33−41.
(30) Evangelio, E.; Ruiz-Molina, D. *Eur. J. Inorg. Chem.* **2005**, 2957−2971. Sato, O.; Tao, J.; Zhang, Y.-Z. *Angew. Chem., Int. Ed.* **2007**, *46*, 2152−2187.
(31) Shimazaki, Y.; Tani, F.; Fukui, K.; Naruta, Y.; Yamauchi, O. *J. Am. Chem. Soc.* **2003**, *125*, 10512−10513. Shimazaki, Y.; Kabe, R.; Huth, S.; Tani, F.; Naruta, Y.; Yamauchi, O. *Inorg. Chem.* **2007**, *46*, 6083−6090.
(32) Rotthaus, O.; Thomas, F.; Jarjayes, O.; Philouze, C.; Saint-Aman, E.; Pierre, J.-L. *Chem.−Eur. J.* **2006**, *12*, 6953−6962.

(33) Dewer, M. J. S.; Talati, A. M. *J. Am. Chem. Soc.* **1963**, *85*, 1874. Dewer, M. J. S.; Talati, A. M. *J. Am. Chem. Soc.* **1963**, *86*, 1592−1595.
(34) Kuhnert, N.; Lopez-Periago, A.; Rossignolo, G. M. *Org. Biomol. Chem.* **2005**, *3*, 524−537. Kuhnert, N.; Rossignolo, G. M.; Lopez-Periago, A. *Org. Biomol. Chem.* **2003**, *1*, 1157−1170.
(35) Ronald, R. C.; Winkle, M. R. *Tetrahedron* **1983**, *39*, 2031−2042.

SCHEME 2. Synthesis of 3
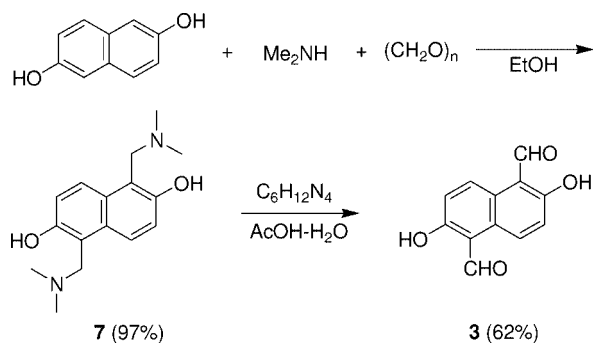
2,6-dihydroxynaphthalene-1,5-dicarbaldehyde (**3**), 3,7-dihydroxynaphthalene-2,6-dicarbaldehyde (**4**), and bis(2,6-dihydroxy-7-formylnaphthyl)methane (**6**), while 2,6-dihydroxynaphthalene-1,7-dicarbaldehyde (**5**) could not be identified. The poor regioselectivity observed here agreed with previous results reported for the formylation of hydroxynaphthalene under similar conditions.[6,36] After tedious separation, 1−10% yields of each compound were obtained.

Since the above method gave **3** quite a poor yield and the separation of **3** from **4** was difficult, we used a second approach to synthesize **3**. In this method (Scheme 2), the condensation of 2,6-dihydroxynaphthalene, paraformaldehyde and dimethylamine in ethanol gave a Mannich base (**7**), which was allowed to react with hexamethylenetetramine.[37,38]

Solid-State Structure. Slow evaporation of a solution of **3** in toluene produced a single crystal suitable for X-ray structural analysis. Similarly, a single crystal of **4** was obtained from its DMF solution. Parts a and b of Figure 2 show the ORTEP drawings of **3** and **4**, respectively. Since **3** and **4** formally represent fused salicylaldehydes, their hydroxy groups intrinsically have a phenol−aldehyde/quinoid−enol tautomeric character. For **3** and **4**, the C−O(H) bond distances were 1.345 and 1.370 Å, respectively, which are more likely to be phenolic C−O bond lengths than keto C=O bond. Moreover, the C−C(=O) bond distances were 1.450 and 1.456 Å, respectively, in a range of typical aromatic aldehyde bond lengths. Therefore, we concluded that the salicylaldehyde moieties of **3** and **4** adopted a phenol−aldehyde form in the crystal state. Since the lengths of these bonds are closely related to the strength of hydrogen bond,[39] we later discuss them in more detail.

On modeling the crystal structure of **3**, we assumed the formation of an intramolecular hydrogen bond between formyl and hydroxy groups, in view of the substantial planarity of O=C−C−C−O moiety (dihedral angle of O=C−C−C is −5.25°), and the proximity of two oxygen atoms (O---O distance is 2.593 Å). For **4** as well, we assumed the formation of a similar intramolecular hydrogen bond, based on the substantial planarity of the O=C−C−C−O moiety (the dihedral angle of O=C−C−C is 2.92°) and the proximity of two oxygen atoms (O---O distance is 2.71 Å). These geometrical parameters are similar to those observed for their analogous compounds that have intramo-
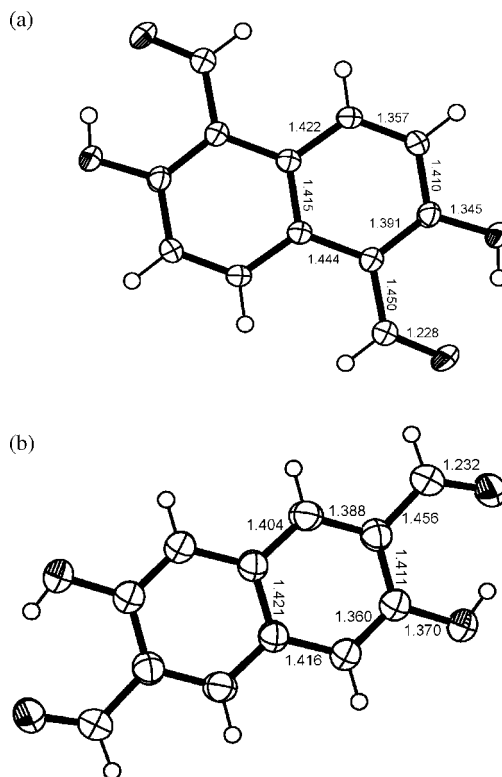

FIGURE 2. ORTEP drawings of the crystal structure of (a) **3** and (b) **4**. Selected bond lengths in angstroms.
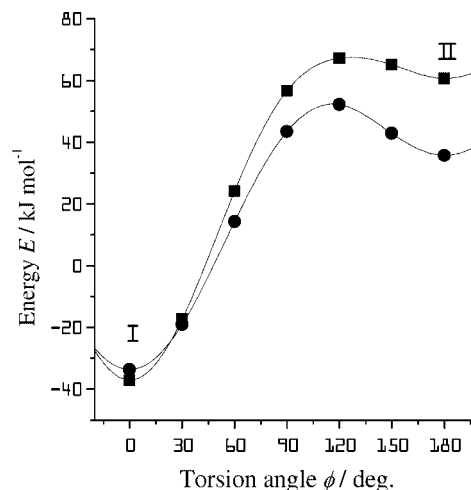

FIGURE 3. Potential curves of **3** and **4** as functions of the torsion angle ϕ of the C(CHO)−C−O−H moiety. $\phi = 0°$ indicates the closed form of the salicylaldehyde unit.

lecular hydrogen bond.[40] IR spectra of **3** and **4** gave significantly broadened peaks at 3432 and 3302 cm^{-1}, respectively, which are attributable to the stretch vibration of intramolecularly hydrogen-bonded hydroxy groups.

To support the validity of assumed intramolecular hydrogen bonds, we performed ab initio molecular orbital calculations. Figure 3 shows potential curves of **3** and **4** as a function of the torsion angle ϕ of C(CHO)−C−O−H framework, where ϕ is defined as 0° when the proton-bridged quasi ring is closed. The curves are plotted against simultaneous and synchronous change

(36) Harvey, R. G.; Cortez, C.; Ananthanarayan, T. P.; Schmolka, S. *J. Org. Chem.* **1988**, *53*, 3936−3943.

(37) Kuriakose, A. P.; Sethna, S. *J. Ind. Chem. Soc.* **1966**, *43*, 437−439. Kuriakose, A. P. *Indian J. Chem.* **1975**, *13*, 1149−1151.

(38) Tamura, K.; Kato, Y.; Ishikawa, A.; Kato, Y.; Himori, M.; Yoshida, J.; Takashima, Y.; Suzuki, T.; Kawabe, Y.; Cynshi, O.; Kodama, T. *J. Med. Chem.* **2003**, *46*, 3083−3093.

(39) Krygowski, T. M.; Zachara-Horeglad, J. E.; Palusiak, M.; Pelloni, S.; Lazzeretti, P. *J. Org. Chem.* **2008**, *73*, 2138−2145.

(40) Fernández-G, J. M.; Espinosa-Pérez, G. *J. Chem. Crystallogr.* **1994**, *24*, 151−154.
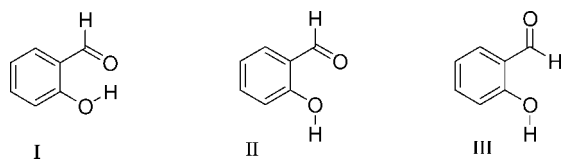
**FIGURE 4.** Notation of the conformers of salicylaldehyde: (I) closed, (II) *Z*-open, and (III) *E*-open.
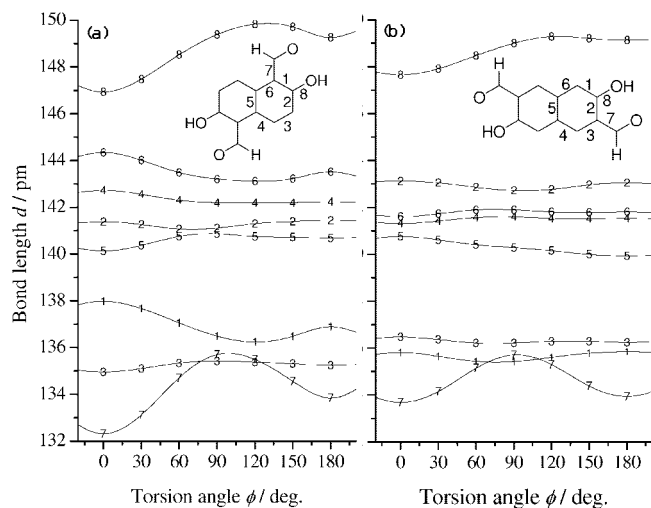
FIGURE 5. Calculated bond lengths of **3** and **4** as functions of the torsion angle ϕ.

in two ϕ angles. The energy is calculated by reference to that of the *E*-open form (III in Figure 4) of the salicylaldehyde moiety. Namely, the energy difference between two potential minima at $\phi = 0°$ and $\phi = 180°$ corresponds to the energy difference for an adiabatic open/close process of the intramolecular hydrogen bond. The figure implies overwhelming stability of the closed form (I in Figure 4) against the *Z*-open form (II). It is thus reasonable to assume intramolecular hydrogen bonding for these systems. The origin of a sizable difference (97.7 kJ/mol for **3** and 69.4 kJ/mol for **4**) in the stabilization energy is discussed later.

Parts a and b of Figure 5 plot the calculated interatomic distances of C–C and C–O bonds in **3** and **4**, respectively, as functions of ϕ defined above. Figure 5 clearly shows that the formation of the intramolecular hydrogen bond brings about considerable changes in bond length all over the naphthalene ring. For both **3** and **4**, the C–CHO bond (denoted as 7) and the C–OH bond (denoted as 8) shortened on going from open to closed form. Simultaneously, the bond (denoted as 1 for **3** and as 2 for **4**) between carbons substituted by formyl and hydroxy groups elongated. The trend of those changes is understandable in view of the resonance hybrid involving the covalent and ionic structures of each salicylaldehyde moiety (Scheme 3). As compared to **4** (Scheme 3B), the structure of **3** (Scheme 3A) has a larger number of possible resonance structures involving ionic structures, responsible for more prominent change in the bond length. In other words, the calculated bond lengths well reflect the changes in resonance structure that were induced by the intramolecular hydrogen bonding. Further, the observed difference in the length of each bond between **3** and **4** is plotted against the one calculated for $\phi = 0°$ (Figure 6). There is an excellent correlation between calculated (Δd_{calcd}) and observed (Δd_{obsd}) values of the difference in bond length, suggesting that the present calculations can qualitatively (at least relatively) reproduce the effects of formyl

SCHEME 3. Resonance structures of 3 (A) and 4 (B)
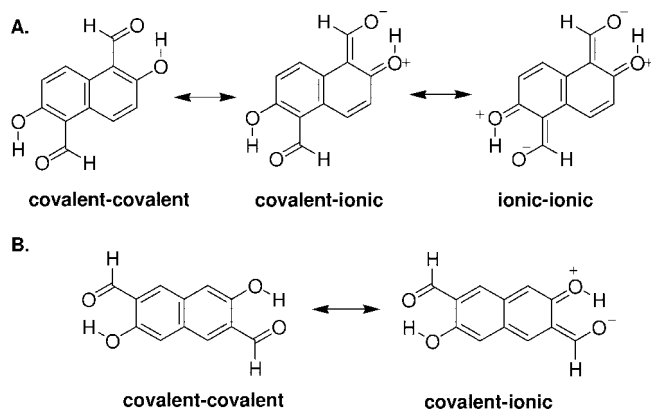
groups at different positions on the electronic state of naphthalene's π-system.

**Solution-State Structure.** ^{1}H NMR spectra of **1**−**5** were measured in DMSO-d_6. The −OH protons resonated at about 11.6 ppm when positioned ortho to an α-formyl group and were in the range of 10.2−10.5 ppm when positioned ortho to a β-formyl group. These characteristic downfield shifts suggest that intramolecular hydrogen bonding was maintained even in the polar dimethyl sulfoxide solvent. The chemical shift of the −OH protons of the α- and β-formyl derivatives differed by more than 1 ppm, and the chemical shifts (10.2−10.5 ppm) of −OH protons neighboring β-formyl groups were rather close to those ($\sim$9.7 ppm) observed for hydrogen-bond-free −OH protons. Such a difference in downfield shift implies that an α-formyl group serves as stronger hydrogen bond acceptor than does a β-formyl group.

The potential surface (Figure 3) of **3** and **4** with respect to the rotation of the C(CHO)−C−O−H moiety suggests that the main conformers present in solution are types of I−I, I−III, and III−III, where I and III means the partial conformation of salicylaldehyde unit denoted in Figure 4. To more quantitatively discuss the solution-state structure of the compounds, we performed an ab initio magnetic shielding calculation by using the GIAO (gauge invariant atomic orbital) method, which is widely used to interpret the magnetic properties of organic compounds including π-conjugated systems.[41] Figure 7 shows the ^{13}C chemical shift of the naphthalene carbons subtracted
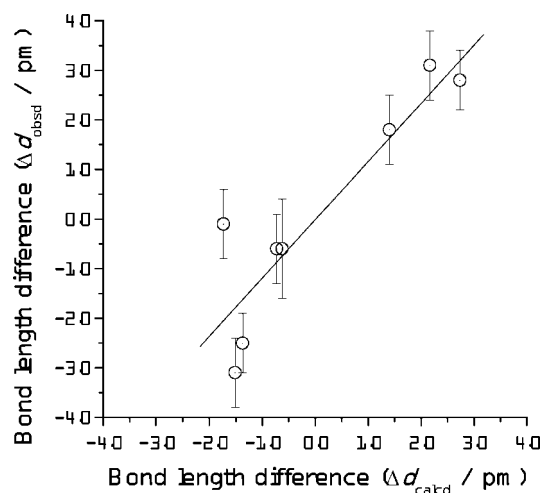
FIGURE 6. Correlation between the calculated and observed values of the bond length difference between **3** and **4**.
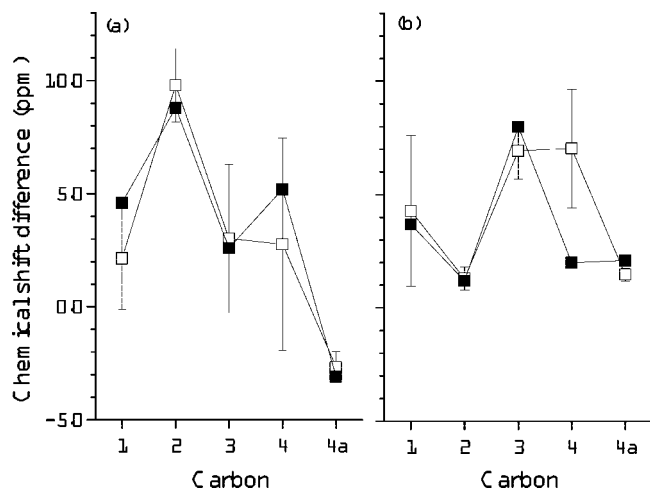
FIGURE 7. Observed (solid symbols) and calculated (open symbols) of the chemical shifts of naphthalene carbons of (a) **3** and (b) **4** by reference to those of 2,6-dihydroxynaphthalene.

by that of the corresponding carbons of 2,6-dihydroxynaphthalene so that these values could represent the effect of formyl substitution in each compound. For convenience of comparison, the carbons are numbered by regarding **4** as 2,6-dihydroxynaphthalene-3,7-dicarbaldehyde. The observed values (solid symbols) exhibited sizable downfield shift for carbons C1, C2, and C4 of **3** and C1 and C3 of **4**. The calculated values (open symbols) are the equally weighted average of the shielding constants for the conformers I−I ($\phi = 0°$ and $\pm 30°$) and III−III. The error bars indicate the standard deviation of the calculated values with respect to the conformational change. We have also confirmed that the conformer I−III simply gave an arithmetic average of I−I and III−III results. The calculation revealed that the shielding constants of carbons C3 and C4 of **3** vary largely depending on the conformational change, and the equally weighted average moderately reproduces the observed value. The conformation dependence of the calculated shielding constants of **4** is relatively small, and again, the equally weighted average well reproduces the observed values except carbon C4. The attempt of taking into account other conformers, for example, II−II, did not improve the fitting between observed and calculated values. Consequently, the overall agreement between observed and calculated chemical shifts suggests that in solution **3** and **4**, respectively, are present as an equilibrium mixture of the conformers I−I, I−III, and III−III, which convert to each other on a relatively flat potential surface.

Effects of RAHB on the Adjoining π-System. In the previous section, Figure 5 suggested that the rotation of the C(CHO)−C−O−H moiety considerably affects the equilibrium distance of C−C and C−O bonds in **3** and **4**. The changes in bond lengths are quite informative in connection with a geometrical criterion of local aromaticity. The harmonic oscillator model of aromaticity (HOMA) index is defined as a normalized variance of the bond lengths by reference to a length optimum for ideal aromatic system. For evaluation of the HOMA index, we utilized eq 1, where $R_{opt} = 1.388$ Å and $\alpha = 257.7$, as proposed by Kruszewski and Krygowski.[42] Several studies have shown that the HOMA index finely correlates with
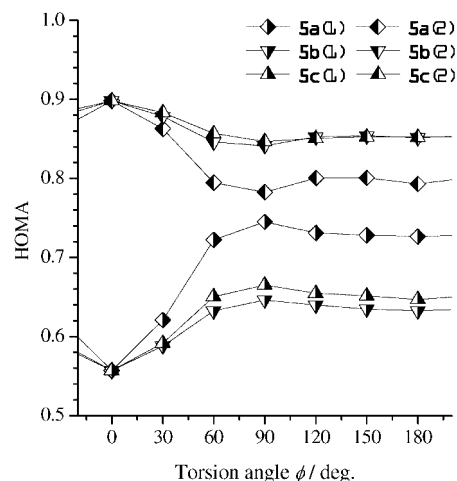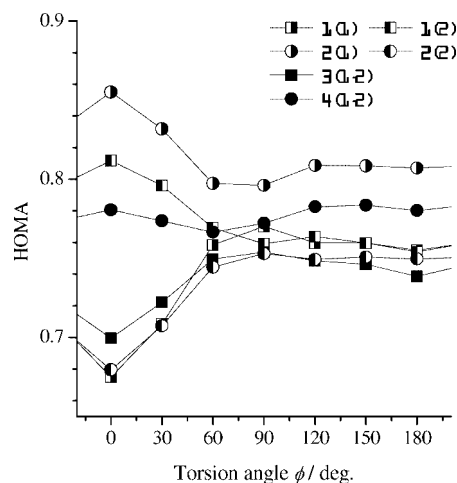
FIGURE 8. HOMA index of the individual local ring denoted in Figure 9 as a function of ϕ.

other geometry-based and magnetism-based criteria of aromaticity.[25,43−48] For naphthalene system, a special interest is addressed to position-dependent substituent effects on aromaticity.[49,50]

$$\text{HOMA} = 1 - \frac{\alpha}{n}\sum_{i=1}^{n}(R_{opt} - R_i)^2 \qquad (1)$$

Figure 8 plots HOMA indices of local six-membered rings of **1**−**5** as functions of ϕ. The numbering of rings and the C−O bond(s) that rotate(s) are given in Figure 9. For **1**, the closure of the proton-bridged quasi-ring induces the decrease of aromaticity in the formyl-substituted ring (**1**(1)) and increase of aromaticity in the other ring (**1**(2)). This result indicates that **1** in the closed form is preferably drawn as a structure like I in

(41) Facelli, J. C., de Dios, A. C., Eds. *Modeling NMR Chemical Shifts−Gaining Insight into Structure and Environment*; American Chemical Society: Washington, DC, 1999.
(42) Kruszewski, J.; Krygowski, T. M. *Tetrahedron Lett.* **1972**, *36*, 3839−3842.

(43) Grabowski, S. J. *J. Phys. Org. Chem.* **2003**, *16*, 797−802.
(44) Palusiak, M.; Simon, S.; Solà, M. *J. Org. Chem.* **2006**, *71*, 5241−5248.
(45) Palusiak, M.; Krygowski, T. M. *Chem.−Eur. J.* **2007**, *13*, 7996−8006.
(46) Krygowski, T. M.; Zachara, J. E.; Ośmiałowski, B.; Gawinecki, R. *J. Org. Chem.* **2006**, *71*, 7678−7682.
(47) Mohajeri, A. *THEOCHEM* **2004**, *678*, 201−205.
(48) Zborowski, K.; Proniewicz, L. M. *J. Phys. Org. Chem.* **2008**, *21*, 207−214.
(49) Krygowski, T. M.; Palusiak, M.; Plonka, A.; Zachara-Horeglad, J. E. *J. Org. Phys. Chem* **2007**, *20*, 297−306.
(50) Fiarowski, A.; Kochel, A.; Kluba, M.; Komounah, F. S. *J. Org. Phys. Chem.* **2008**, *21*, 939−944.
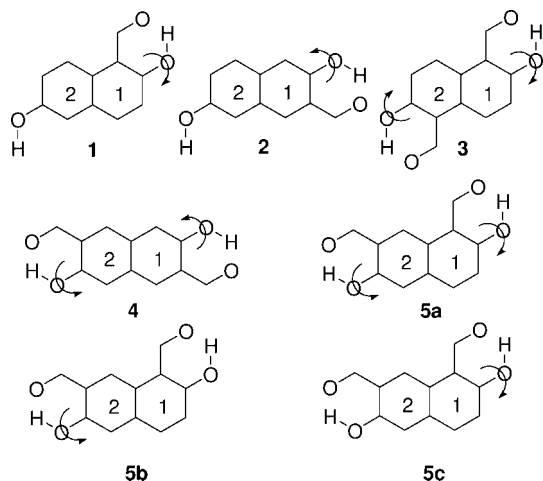
FIGURE 9. Numbering of the local six-membered rings of **1**−**5**. Arrows indicate the bonds that rotate as ϕ changes from 0° (tail) to 180° (head).
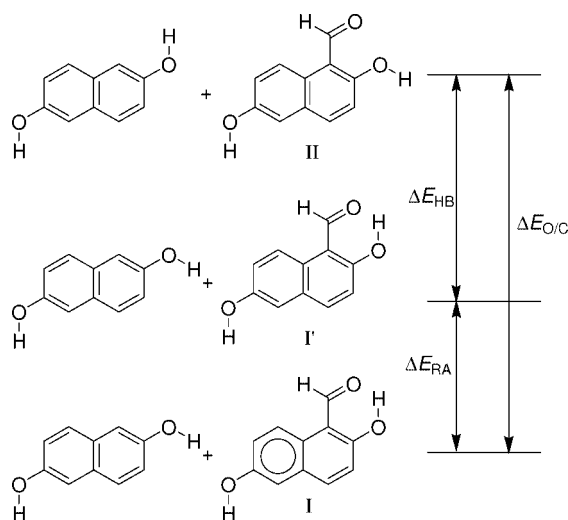

FIGURE 10. Hypothetical energy diagram to evaluate the strength of RAHB.

Figure 10 using Clar's π-sextet model.[51] Interestingly, for **2**, the trend of change in HOMA index is totally opposite to **1**; namely, the closing of the proton-bridged quasi ring induces the increase of aromaticity in the formyl-substituted ring (**2**(1)) and decrease of aromaticity in the other ring (**2**(2)). Similar results have already reported by Palusiak et al.,[44] but the present case is much more prominent maybe because of the participation of 6-hydroxy group to the π-electron resonance.

Further, the results of **3** and **4** highlight the interference effect of the RAHB. For **3**, the closing of the proton-bridged quasi ring induces the decrease of aromaticity in both rings of **3**(1) and **3**(2), and their HOMA index is as small as that of **1**(1) ring. On the contrary, for **4**, the closure of the quasi ring hardly changes the aromaticity of both rings of **4**(1) and **4**(2), and their HOMA index is similar to that for the *Z*-open (i.e., II−II) form. This equalization of aromaticity corresponds to the character of a migrating π-sextet system. The above results may be also interpreted based on the resonance hybrid structure shown in Scheme 3. For **3**, we can draw any of the covalent−covalent, covalent−ionic, and ionic−ionic structures. Namely, two sali-

(51) Randić, M. *Chem. Rev.* **2003**, *103*, 3449−3605.
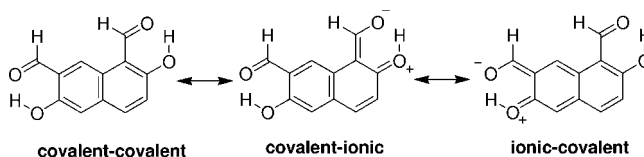
SCHEME 4

SCHEME 5
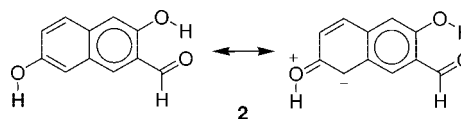
cylaldehyde units can be treated as if they were independent. On the other hand, for **4**, we can only draw either covalent−covalent or covalent−ionic structures. The contributions of the ionic structure from each half are exclusive, and hence, two salicylaldehyde units are not independent. As a consequence of interference between the contributions of ionic structure of two salicylaldehyde units, **3** undergoes a decrease of aromaticity in the both ring, while **4** undergoes the compensation of aromaticity in the both ring. Upon comparison to an electric circuit, the RAHB units of **3** work as switches of two independent circuits, whereas the RAHB units in **4** work as inputs of XOR logic gate.

Based on the above results, we can expect **5** to exhibit an extreme imbalance of aromaticity over the two local rings. Indeed, the closing of the quasi ring increases the HOMA index of the ring **5a**(1) up to 0.90 and decreases that of **5a**(2) down to 0.56. Further, we examined two cases illustrated as **5b** and **5c**. Interestingly, the HOMA indices of the rings **5b**(1) and **5c**(1) showed almost the same dependence on ϕ, and so did the rings **5b**(2) and **5c**(2). These results suggest that the closure of either quasi ring attached to the ring 1 or 2 makes the ring 1 reach the highest level of aromaticity and makes the ring 2 reach the lowest level of aromaticity. This phenomenon may also correspond to the resonance hybrid formula (Scheme 5) of **5**, where we can see the contributions of ionic structure from two salicylaldehyde units are exclusive. Consequently, for **5** the RAHB units work as inputs of OR logic gate.

The above results may give us a possible interpretation for the composition of the products shown in Scheme 1: **5** was not obtained and the yield of **2** was poor. For **2**, the C5-carbon assumes a negative charge, because the C5−C6−OH moiety has an isolated enol-like character, since the formyl-substituted ring can be represented as a π-sextet with high aromaticity (Scheme 5). For **5**, on the other hand, the formyl group will show high reactivity due to its isolated enal-like character. These compounds may have suffered some coupling reactions to give unidentifiable oligomers or polymers. A minor product **6** appears given by the cross-coupling of **2** and **5**, which occurred somewhere during the reaction procedure.

Since the origin of the stabilization of RAHB is electronic delocalization along the proton-bridged quasi-six-membered ring, the naphthalene's π-system simultaneously undergoes electronic donation from the hydroxy group and electronic withdrawing from the formyl group. Namely, the effect of resonance-assist can be interpreted as a stabilization energy that is caused by mixing of the ionic state wave function into the covalent state wave function. Therefore, the stabilization of the hydrogen bond on the one hand would cause destabilization by the loss of aromaticity on the other hand. If such an energetic

TABLE 1. List of Calculated Energies Related to the Diagram in Figure 10^a

	I	II	III	$\Delta E_{O/C}$	ΔE_{HB}	ΔE_{RA}
1	(0.0)	50.9	36.2	46.8	37.9	8.9
	(0.0)	58.8	42.7	56.1	44.1	12.0
2	(0.0)	35.2	17.6	39.3	32.8	6.4
	(0.0)	41.7	28.3	44.4	35.3	9.1
3	(0.0)	97.7	37.1	89.6	70.6	19.0
	(0.0)	114.7	57.4	109.6	85.8	23.8
4	(0.0)	69.4	33.6	77.5	64.8	12.7
	(0.0)	82.1	54.5	87.2	69.4	17.8
5	(0.0)	86.4	47.1	86.4	69.9	16.5
	(0.0)	100.5	67.5	100.5	79.1	21.4

^{a} Upper and lower rows contain HF/6-311G(d,p) and B3LYP/6-311G(d,p)//HF−311G(d,p) results, respectively.

"tradeoff" results in a net decrease in aromaticity, it suggests the predominance of the resonance-assisted effect. On comparing the aromaticity of **3** and **4** in Figure 8, we can expect **3** to have a larger contribution of resonance-assist to the intramolecular hydrogen bond.

In Figure 3, we demonstrated the energy differences for **3** and **4** are 97.7 and 64.8 kJ/mol, respectively, suggesting an overwhelming thermodynamic stability of closed form of **3**. However, the total amount of energy difference between closed (I−I) form and open (II−II) form is not simply a measure of the strength of RAHB.[43,44] To clarify the contents of the energy difference, first we defined $\Delta E_{O/C}$ as a net energy necessary to open the closed quasi ring by using a hypothetical diagram (Figure 10) to eliminate the effects of intrinsic conformational preference of hydroxy groups. Next, we calculated the energy of the structure I′ that was built by changing only the dihedral angles of formyl and hydroxy groups to close a proton-bridged quasi ring with the other geometry remaining unchanged from structure II. Then we divided $\Delta E_{O/C}$ into (i) net stabilization of hydrogen bonding (ΔE_{HB}) and (ii) resonance-assisted stabilization (ΔE_{RA}), according to the diagram in Figure 10. Therefore, the following relation holds.

$$\Delta E_{OC} = \Delta E_{HB} + \Delta E_{RA} \qquad (2)$$

The ΔE_{RA} value is reported to show fairly good correlation with an aromaticity index based on Bader's theory.[45] It should be noted that the ΔE_{HB} value does not purely reflect the hydrogen-bonding energy because it includes O---O repulsion in the open structure. However, in the present case, difference in the repulsion energy among **1−5** can be neglected in view of the similarity of their local structures.

Table 1 lists the values of energy of conformers II and III relative to that of I (for compounds **3**, **4**, and **5** the notation I implies I−I and so on). The results from Hartree−Fock (HF) calculation (upper rows) of **1−5** indicate that ΔE_{HB} occupies about 80% (78.8−83.6%) of $\Delta E_{O/C}$ and that both ΔE_{HB} and ΔE_{RA} of α-formyl derivatives are greater than those of β-formyl derivatives. Interestingly, additivity roughly holds among ΔE_{HB} (and naturally ΔE_{RA} as well) values of the compounds. The values of ΔE_{HB} per hydrogen bond are 37 kJ/mol for the quasi rings including α-formyl group and 33 kJ/mol for the quasi rings including β-formyl groups, respectively. Similarly, the values of ΔE_{RA} per hydrogen bond are 9 kJ/mol for the quasi rings including α-formyl group and 6 kJ/mol for the quasi rings including β-formyl groups, respectively. The DFT calculation (B3LYP, lower rows) gave results similar to those from HF calculation, although each value of the former is 1.1−1.2 times

as large as the latter. These results are in agreement with a prediction based on the discussion of the change in aromaticity, although the difference in the resonance-assisted effect among **1−5** was smaller than expected. Rather, difference in ΔE_{HB} could contribute more critically to $\Delta E_{O/C}$.

UV−vis Spectra. Figure 11 shows the ultraviolet−visible (UV−vis) absorption spectra of **1−4** and **6**. Moderately intense bands appeared in the regions of 280−330 nm (region I) and 350−550 nm (region II); these bands are attributable to $\pi\pi^*$ transitions, and the bands in the longer wavelength region are characteristic of carbonyl-bearing naphthalene systems.[52−57] The spectra of the α-formyl derivatives **1** and **3** were similar to each other, but the values of the molar absorption coefficient ε of **3** (14300 M^{-1} cm^{-1} at 319 nm and 7800 M^{-1} cm^{-1} at 404 nm) were roughly twice as large as those of **1** (7900 M^{-1} cm^{-1} at 320 nm and 5000 M^{-1} cm^{-1} at 388 nm). For **2**, a β-formyl derivative, the peak observed in region II, at 414 nm, was significantly broadened and red-shifted compared to the peak observed for **1**, an α-formyl derivative. A peak similar to **2** was also observed at 425 nm for **6**, indicating that such relatively red-shifted peaks were characteristic of β-formyl derivatives. For **4**, the β-diformyl derivative, the region II peak was even more red-shifted, to 476 nm, and the absorbance of the region I peak (314 nm) was about twice as intense as that observed for any of the other derivatives. These spectral features were similar to those observed for naphthalene monocarbaldehydes.[56,57] The absorption maxima of **1** and **2** were red-shifted by ~30−40 nm with respect to that of 1- and 3-formyl-2-naphthols, respectively, and this red shift was interpreted as an electron donating effect of the OH groups in *amphi*-positions of **1** and **2**.

We focused on the region II absorption band, which was shifted with varying substitution positions. A considerable difference in absorption maxima between **3** (404 nm) and **4** (476 nm) is of special interest. Since the spectral feature mentioned above is also observed for solid-state samples, the difference in absorption maxima is originating in the molecular structure, not in other environmental factors like solvent effects.

In the previous sections, we revealed several effects of the intramolecular hydrogen bond(s) on the electronic state of the molecules for **1−5**. In addition, analysis on NMR chemical shifts suggested that the intramolecular hydrogen bond is maintained in solution state. The intramolecular hydrogen bond induces a change in electronic state of the naphthalene ring, which is illustrated as a mixing of the ionic state into the covalent state to some extent. For these compounds, the ground-state wave function Ψ_g is represented as $a\Psi_{cov} + b\Psi_{ion}$, where Ψ_{cov} and Ψ_{ion} are the wave functions of covalent and ionic states and a

(52) Fita, P.; Luzina, E.; Dziembowska, T.; Radziewicz, Cz.; Grabowska, A. *J. Chem. Phys.* **2006**, *125*, 184508−184518.
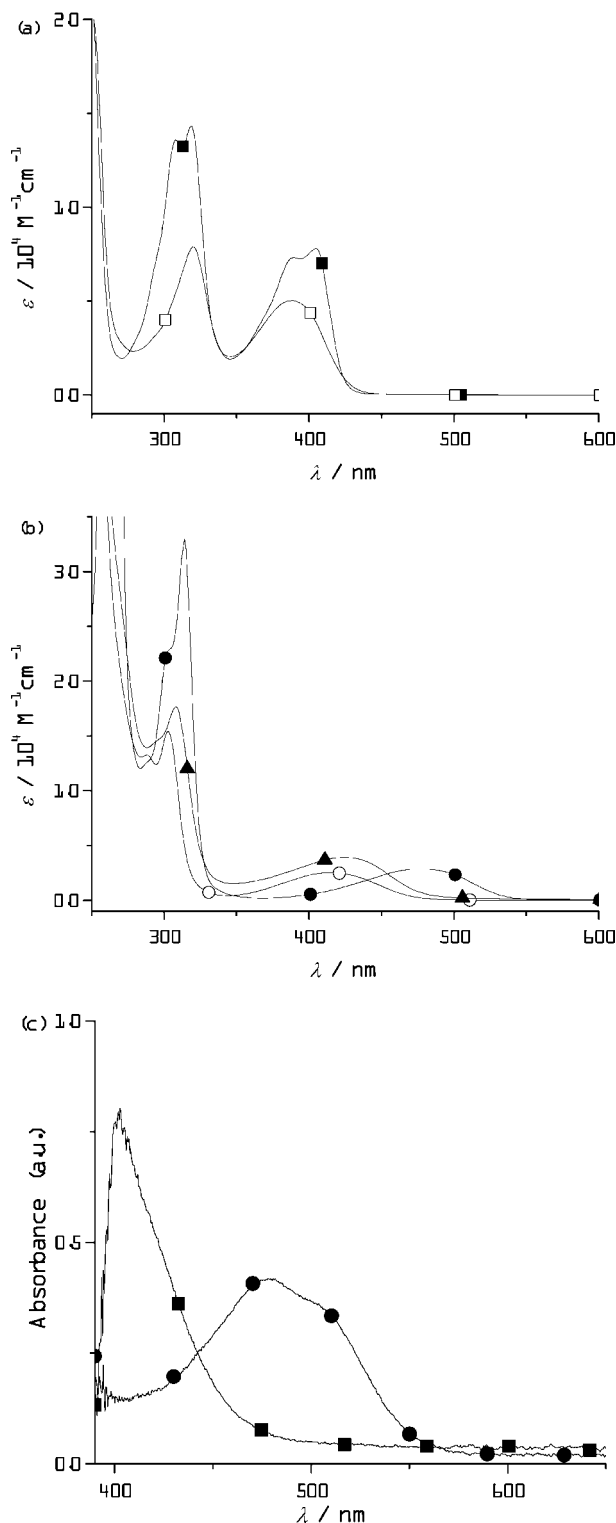
(53) Fabian, W. M. F.; Antonov, L.; Nedeltcheva, D.; Kamounah, F. S.; Taylor, P. J. *J. Phys. Chem. A* **2004**, *108*, 7603−7612. Antonov, L.; Fabian, W. M. F.; Nedeltcheva, D.; Kamounah, F. S. *J. Chem. Soc. Perkin Trans. 2* **2000**, 1173−1179.

(54) Oshima, A.; Momotake, A.; Arai, T. *J. Photochem. Photobiol.* **2004**, *162*, 473−479. Oshima, A.; Momotake, A.; Arai, T. *Chem. Lett.* **2005**, *34*, 1288−1289.

(55) Alarcón, S. H.; Olivieri, A. C.; Labadie, G. R.; Cravero, R. M.; González-Sierra, M. *Tetrahedron* **1995**, *51*, 4619−4626.

(56) Chowdhury, P.; Chakravorti, S. *Chem. Phys. Lett.* **2004**, *395*, 103−108. Chowdhury, P.; Panja, S.; Chakravorti, S. *J. Phys. Chem. A* **2003**, *107*, 83−90. Adhikary, T. P.; Chowghury, P.; Chakravorti, S. *Chem. Phys. Lett.* **2007**, *442*, 504−510.

(57) Mahanta, S.; Singh, R. B.; Kar, S.; Guchhait, N. *Chem. Phys.* **2006**, *324*, 742−752. Singh, R. B.; Mahanta, S.; Kar, S.; Guchhait, N. *Chem. Phys.* **2007**, *331*, 373−384.

TABLE 2. Lowest Energy Absorption Wave Lengths (λ/nm) Calculated by the TD DFT Method

	I	I′	II	III	obsd
1	353.6	353.7	344.7	352.5	388
2	399.9	396.4	362.7	371.2	414
3	360.2	359.3	355.8	354.7	404
4	469.5	461.1	402.1	409.0	476
5	403.8	404.4	374.9	376.0	

8) and the resonance assist effect ΔE_{RA} (Table 1), the contribution of the ionic state to the ground state is greater for **3** than for **4**. This means that **3** has a relatively greater value of the coefficient *b*, responsible for the lowering of the ground-state level as compared to that of **4**. This model can give a qualitative explanation for a substantial difference in absorption maxima between **3** and **4**.

For a more quantitative discussion of the excitation energy, we performed a TD (time-dependent) DFT calculation using B3LYP functional.[58] The calculated wavelengths of the lowest energy absorption are summarized in Table 2. The columns I, II, and III contain a value calculated for the corresponding structure, i.e., closed, *Z*-open, and *E*-open forms (see Figure 4) (again, for compounds **3**, **4**, and **5** the notation I implies I−I, and so on). The structure I′ is the same structure as mentioned in Figure 10.

Based on the results in Table 2, we can explain the data of absorption maxima observed for **1**−**4**. Each data column of I, II, and III is fairly correlated with the observed data (the right column). Since the solution-state structures of **3** and **4** were identified as an equilibrium mixture of the structures I−I, I−III, and III−III, it seems natural to consider a similar equilibrium for the other compounds. Relatively small differences (1−6 nm) between columns I and III for **1** and **3** are in agreement with sharp peaks observed for these compounds. On the other hand, a sizable difference (30−60 nm) for **2** and **4** account for the broad absorption bands observed around 414 and 476 nm, respectively.

Comparison of the columns of I and II suggests that the formation of an intramolecular hydrogen bond would result in a significant red shift of the absorption maxima. The columns of I and I′, both of which have closed form, show only a slight difference, indicating that the red shift was induced by the closure of the quasi ring(s), not by the distortion of the naphthalene ring. The absorption wavelengths calculated for the structure III are more or less similar to those for II, which confirms that the intramolecular hydrogen bond is responsible for the red shift. Interestingly, the amounts of the red shift on going from II to I is prominent for **2** (2565 cm^{-1}), **4** (3570 cm^{-1}), and **5** (1909 cm^{-1}), as compared to those of **1** (730 cm^{-1}) and **3** (343 cm^{-1}). These values show negative correlation with the ΔE_{RA} value that represents the amount of stabilization energy by resonance effect of RAHB (see Table 1). Consequently, the order of the red shift is explained as follows. The intramolecular hydrogen bond forms a proton-bridged quasi ring, to which π-electrons of the naphthalene ring delocalize according to the resonance hybrid scheme (Schemes 3 and 4). The mixing of the naphthalene's and the quasi ring's π-systems leads to the elevation of HOMO and the lowering of LUMO, resulting in red shift of $\pi\pi^*$ transition. In case the hydrogen bonding in the

FIGURE 11. UV−vis spectra of the 2,6-dihydroxynaphthalene carbaldehydes: **1** (□), **2** (○), **3** (■), and **4** (●). Solution-state (in CHCl₃) spectra of (a) α-formyl-bearing compounds (**1** and **3**) and (b) β-formyl-bearing compounds (**2**, **4**, and **6**). (c) Solid-state spectra of **3** and **4** measured for thin films smeared on a slide glass.

and *b* are mixing coefficients, and we can straightforwardly find the excited-state wave function Ψ_e to be $b\Psi_{cov} - a\Psi_{ion}$. According to this two-state model, the excitation energy directly reflects the stability of the ground state, since the energies of the ground and excited states symmetrically vary depending on the mixing coefficients. In view of the change in HOMA (Figure

(58) Jacquemin, D.; Perpète, E. A.; Scalmani, G.; Frisch, M. J.; Kobayashi, R.; Adamo, C. *J. Chem. Phys.* **2007**, *126*, 144105−144112. Perpète, E. A.; Wathelet, V.; Preat, J.; Lambert, C.; Jacquemin, D. *J. Chem. Theory Comput.* **2006**, *2*, 434−440.
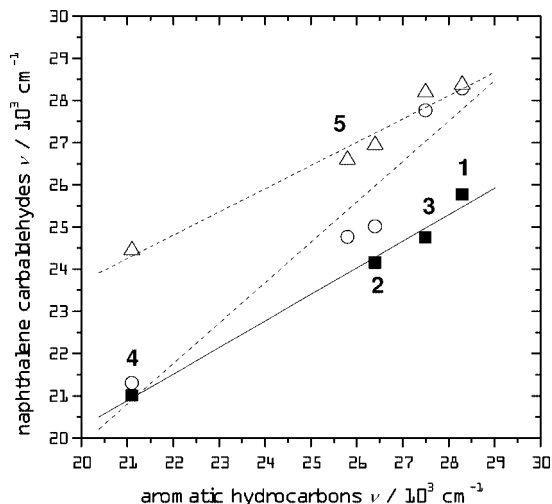
FIGURE 12. Comparison of the lowest energy absorptions of naphthalene carbaldehydes **1−4** plotted against those of their isotopological cata-condensed aromatic hydrocarbons: observed (closed square), calculated for form I (open circle), and calculated for form III (open triangle).

quasi ring is stabilized by the mixing of the ionic state to the ground (covalent) state, the energy level of π-electron is lowered according to the degree of the mixing. The degree of the mixing is determined by tradeoff relation between the stabilization of hydrogen bond and the destabilization due to loss of aromaticity, and their optimal balance depends on a topology of the substituted molecule.

Practically, it might be possible to regard the quasi ring of an RAHB as an additional aromatic ring in view of its delocalized π-electron's nature. Then, the above discussion is reminiscent of the relationship between the absorption maxima and connecting topology for a series of cata-condensed aromatic hydrocarbons.[59] Figure 12 plots the observed and calculated values of the lowest energy absorption of **1−5** as functions of the lowest energy absorption peaks of their isotopological cata-condensed hydrocarbons, namely phenanthrene, anthracene, chrysene, naphthacene, and benz[*a*]anthracene, in this order. A good correlation was observed between the absorptions of **1−5** and those of the hydrocarbons, although the experimental value for **5** is lacking for the moment. This correlation strongly supports the above interpretation of spectral variation based on the RAHB concept. Thus, it is helpful to regard the proton-bridged quasi rings in **1−5** as additional aromatic rings when we consider the electronic state of these molecules.

Conclusions

In summary, we prepared five mono- and diformyl derivatives of 2,6-dihydroxynaphthalene and interpret differences in their structural and spectroscopic aspects by means of ab initio calculations. The difference in the crystal structures between **3** and **4** was successfully explained by the substituent effects. Ab initio calculations revealed that the formation of the intramolecular hydrogen bond considerably influences the bond lengths of naphthalene ring, and the trend of the change was understandable from the conventional schemes of resonance hybrid. The analysis of the observed and calculated NMR chemical shifts implied that the compounds are present as an equilibrium

mixture of the closed form and *E*-open form, and hence, the intramolecular hydrogen bond is partially maintained in solution state. Difference in the thermodynamic stability of the intramolecular hydrogen bond among the compounds studied was also discussed in terms of the resonance-assist mechanism. It was found that the aromaticity of the individual ring of naphthalene changes depended on the topology of substitution of formyl and hydroxy groups, and the trend of the change was again compatible with resonance hybrid schemes. UV−vis absorption profiles of the compounds were finely reproduced by TD DFT calculations, not only in the wavelength but also in the broadness of peaks. We were able to rationalize the calculated results in view of the change in aromaticity of naphthalene ring, and the stabilization energy corresponding to the resonance assist effect on hydrogen bonding. The calculations clearly showed that the origin of the red shift is electronic delocalization over the RAHB unit, rather than the geometrical distortion of naphthalene ring. Comparison with the absorption maxima of aromatic hydrocarbons clearly demonstrated that the *o*-hydroxyaldehyde moieties of these compounds serve as if they were additional aromatic rings that affect the molecule's electronic state.

To date, only a few studies on 2,6-dihydroxynaphthalene carbaldehydes and their Schiff bases have been presented. To the best of our knowledge, this is the first systematic study of a series of 2,6-dihydroxynaphalene mono- and dicarbaldehydes. Closely related to its *amphi*-naphthoquinone-like resonance structure, 2- and 6-OH groups of 2,6-dihydroxynaphalene carbaldehyde appear to determine the stability of intramolecular hydrogen bonding through a resonance-assisted mechanism. These compounds are potentially applicable to several types of polyimines and their metal complexes.[46] The present study provides a useful guide for designing metal-containing materials that show specific electronic properties. Namely, since a metal chelate unit in such compounds will also act as an imaginary aromatic ring that is fused into a core naphthalene ring, the properties of such compounds could be interpreted by analogy with their isotopological hydrocarbons. Our ongoing studies are aimed at clarifying structure−property relationships for a series of Schiff base complexes.

Experimental Section

General procedures of syntheses and measurements are given in the Supporting Information.

Ab initio calculations were performed using the Gaussian03w program.[60] The geometry of each compound was optimized by means of the HF method using the 6-311G(d,p) basis set. DFT calculations using B3LYP hybrid functionals for exchange-correlation energy terms were done for the thus-obtained geometry. **Synthesis of 2,6-Dihydroxynaphthalene-1-carbaldehyde (1), 3,7-Dihydroxynaphthalene-2-carbaldehyde (2), 3,7-Dihydrox-**

(59) Klevens, H. B.; Platt, J. R. *J. Chem. Phys.* **1949**, *17*, 470–481.

(60) *Gaussian 03, Revision C.02*: Frisch, M. J.; Trucks, G. W.; Schlegel, H. B.; Scuseria, G. E.; Robb, M. A.; Cheeseman, J. R.; Montgomery, J. A., Jr.; Vreven, T.; Kudin, N.; Burant, J. C.; Millam, J. M.; Iyengar, S. S.; Tomasi, J.; Barone, V.; Mennucci, B.; Cossi, M.; Scalmani, G.; Rega, N.; Petersson, G. A.; Nakatsuji, H.; Hada, M.; Ehara, M.; Toyota, K.; Fukuda, R.; Hasegawa, J.; Ishida, M.; Nakajima, T.; Honda, Y.; Kitao, O.; Nakai, H.; Klene, M.; Li, X.; Knox, J. E.; Hratchian, H. P.; Cross, J. B.; Adamo, C.; Jaramillo, J.; Gomperts, R.; Stratmann, R. E.; Yazyev, O.; Austin, A. J.; Cammi, F.; Pomelli, C.; Ochterski, J. W.; Ayala, P. Y.; Morokuma, K.; Voth, G. A.; Salvador, P.; Dannenberg, J. J.; Zakrzewski, V. G.; Dapprich, S.; Daniels, A. D.; Strain, M. C.; Farkas, O.; Malick, D. K.; Rabuck, A. D.; Raghavachari, K.; Foresman, J. B.; Ortiz, J. V.; Cui, Q.; Baboul, A. G.; Clifford, S.; Cioslowski, J.; Stefanov, B. B.; Liu, G.; Liashenko, A.; Piskorz, P.; Komaromi, I.; Martin, R. L.; Fox, D. J.; Keith, T.; Al-Laham, A. M.; Peng, C. Y.; Nanayakkara, A.; Challacombe, M.; Gill, P. M. W.; Johnson, B.; Chen, W.; Wong, M. W.; Gonzalez, C.; Pople, J. A. Gaussian, Inc.: Wallingford, CT, 2004.

ynaphthalene-2,6-dicarbaldehyde (**4**), and 2,6-Dihydroxynaphthalene-1,7-dicarbaldehyde (**5**). Sodium hydride (1.1 g, 45.8 mmol) and chloromethylmethyl ether (3.4 mL, 45.2 mmol) were added to a DMF solution (40 mL) of 2,6-dihydroxynaphthalene (3.2 g, 20 mmol) at −20 °C. The solution was stirred for 4 h at room temperature. The solvent was evaporated, and to the residue was added ca. 50 mL of water. By extraction with dichloromethane from the water phase and subsequent concentration, 2,6-bis-(methoxymethoxy)naphthalene was obtained as a colorless solid (4.36 g, 88%). A diethyl ether solution (80 mL) of the methoxymethyl derivative was cooled to −20 °C, and *n*-butyllithium (ca. 1 M in hexane, 41 mL) was added to the cooled solution over a period of 20 min. The reaction solution was stirred for 8 h. Dimethylformamide (8 mL) was then added to the solution, and the solution was stirred for an additional 13 h at room temperature. Aqueous hydrochloric acid (3 N) was added until the pH of the aqueous layer was 6. The diethyl ether layer was collected and concentrated to precipitate the yellow crystalline solid of 3,7-bis(methoxymethyl)naphthalene-2,6-dicarbaldehyde (**4^{MOM}**). The filtrate was further concentrated, and the resulting crude solid (80%) was separated by column chromatography (hexane/ethyl acetate = 6/4, on silica gel) into a fraction containing **1^{MOM}**, **2^{MOM}**, **4^{MOM}**, and **6^{MOM}** and a fraction containing **1^{MOM}**, **2^{MOM}**, and **3^{MOM}**. Each fraction was treated with a mixture of aqueous hydrochloric acid and ethanol to remove the methoxymethyl group, affording the corresponding 2,6-dihydroxynaphthalenes (>90%). **1**, **2**, **4**, and **6** were purified by column chromatography (chloroform/methanol = 10/1, on silica gel). Isolation of **3** from a mixture of **3** and **4** was not successful. The products were recrystallized from chlorobenzene, as necessity arose. Yields (based on 2,6-bis(methoxymethoxy)naphthalene): **1** (42%), **2** (7%), **4** (10%), **3** + **4** (20%), and **6** (3%).

1: yellow needles (mp 193−194 °C); IR (KBr) 3381 (ν_{O-H}), 3234 (ν_{O-H}), 1626 ($\nu_{C=O}$) cm^{-1}; precise MS (EI+) *m/z* 188.0470 (calcd for **1^{+}** 188.0473); ^{1}H NMR (DMSO-d_6) δ 7.13 (d (2.2 Hz), Ar*H*, 1H), 7.14 (d (9.0 Hz), Ar*H*, 1H), 7.17 (dd (2.6, 9.2 Hz), Ar*H*, 1H), 7.93 (d (9.0 Hz), Ar*H*, 1H), 8.79 (d (9.1 Hz), Ar*H*, 1H), 9.65 (s, O*H*, 1H), 10.75(s, C*H*O, 1H), 11.60 (br, O*H*, 1H); ^{13}C NMR (DMSO-d_6) δ 110.6, 112.7, 118.9, 120.8, 123.7, 125.3, 129.2, 136.9, 153.8, 161.7, 192.6; UV−vis (CHCl$_3$) λ/nm (ε/M^{-1} cm^{-1}) 320 (7900), 388 (5000).

2: yellow needles (mp 185−186 °C); IR (KBr) 3461 (ν_{O-H}), 3240 (ν_{O-H}), 1659 ($\nu_{C=O}$) cm^{-1}; precise MS (EI+) *m/z* 188.0472 (calcd for **2^{+}** 188.0473); ^{1}H NMR (DMSO-d_6) δ 7.15 (dd (2.5, 8.9 Hz), Ar*H*,1H), 7.19 (d (2.36 Hz), Ar*H*, 1H), 7.21 (s, Ar*H*, 1H), 7.64 (d (8.9 Hz), Ar*H*, 1H), 8.13 (s, Ar*H*, 1H), 9.67 (s, ArO*H*, 1H), 10.21 (s, O*H*, 1H), 10.36 (s, C*H*O,1H); ^{13}C NMR (DMSO-d_6) δ 109.9, 110.9, 122.5, 124.1, 127.5, 128.1, 129.9, 132.1, 153.4, 153.6, 192.5; UV−vis (CHCl$_3$) λ/nm (ε/M^{-1} cm^{-1}) 288 (13300), 303 (15400), 414 (2500).

4: red plates (dec around 270 °C); IR (KBr) 3301 (ν_{O-H}), 1659 ($\nu_{C=O}$) cm^{-1}; precise MS (EI+) *m/z* 216.0434 (calcd for **4^{+}** 216.0423); ^{1}H NMR (DMSO-d_6) δ 7.41 (s, Ar*H*, 1H), 8.20 (s, Ar*H*, 1H), 10.42 (s, C*H*O, 1H), 10.46 (s, O*H*, 1H); ^{13}C NMR (DMSO-d_6) δ 112.4, 126.7, 129.2, 131.0, 153.9, 192.0; UV−vis (CHCl$_3$) λ/nm (ε/M^{-1} cm^{-1}) 303 (22800), 314 (33000), 476 (2900).

6: brownish orange needles (dec around 320 °C); IR (KBr) 3275 (ν_{O-H}), 1655 ($\nu_{C=O}$) cm^{-1}; precise MS (EI+) no obvious peak detected. Instead, the condensation product (**8**, see the Supporting Information) with *p*-octyloxyaniline gave FAB MS(+) *m/z* 795.3 (calcd for C$_{51}$H$_{58}$N$_2$O$_6$ + H$^+$ 795.4); ^{1}H NMR (DMSO-d_6) δ 4.67 (s, C*H$_2$*, 2H), 7.08 (s, Ar*H*, 2H), 7.35 (d (8.9 Hz), Ar*H*, 2H), 7.48 (d (9.0 Hz), Ar*H*, 2H), 8.71 (s, Ar*H*, 2H), 10.00 (s, O*H*, 2H), 10.18(s, C*H*O, 2H), 10.20(brs, O*H*, 2H); ^{13}C NMR (DMSO-d_6) δ 20.5, 111.3, 120.9, 122.1, 123.4, 125.9, 127.4, 129.7, 133.0, 150.2, 152.9, 192.6; UV−vis (CHCl$_3$) λ/nm (ε/M^{-1} cm^{-1}) 308 (17600), 425 (4000).

^{1}H NMR for **8** (CDCl$_3$): δ 4.67 (s, C*H$_2$*, 2H), 7.08 (s, Ar*H*, 2H), 7.35 (d (8.9 Hz), Ar*H*, 2H), 7.48 (d (9.0 Hz), Ar*H*, 2H), 8.71 (s, Ar*H*, 2H), 10.00 (s, O*H*, 2H), 10.18(s, C*H*O, 2H), 10.20(brs, O*H*, 2H);

Synthesis of 2,6-Dihydroxynaphthalene-1,5-dicarbaldehyde (3). 1,5-Bis(dimethylaminomethyl)-2,6-dihydroxynaphthalene (**7**) was prepared according to ref 37. Mannich base **7** (6.60 g, 24 mmol) was dissolved in 148 mL of aqueous acetic acid (81 vol%), and 9.45 g (67.5 mmol) of hexamethylenetetramine was added to the solution. The mixture was stirred at 130 °C for 4 h. After the mixture was cooled to room temperature, the precipitate was collected by filtration and washed with methanol. Aqueous hydrochloric acid (72 g, 4.5 N) was added to the filtrate, which was stirred at 90 °C an additional 1.5 h. The resulting precipitate was collected by filtration and recrystallized from chloroform to remove impurities.

3: yellow needles (mp 239−240 °C); IR (KBr) 3432 (ν_{O-H}), 1639 ($\nu_{C=O}$) cm^{-1}; precise MS (EI) *m/z* 216.0433 (calcd for **3^{+}** 216.0423); ^{1}H NMR (DMSO-d_6) δ 7.35 (d (9.4 Hz), Ar*H*, 2H), 9.18 (d (9.4 Hz), Ar*H*, 2H), 10.76 (s, C*H*O, 2H), 11.59 (br, O*H*, 2H); ^{13}C NMR (DMSO-d_6) δ 113.3, 121.3, 125.8, 132.4, 161.5, 192.6; UV−vis (CHCl$_3$) λ/nm (ε/M^{-1} cm^{-1}) 308 (13600), 319 (14300), 389 (7300), 404 (7800). Anal. Calcd for C$_{12}$H$_8$O$_4$: C, 66.67; H, 3.73. Found: C, 66.44; H, 3.59.

Crystallographic Data. For X-ray diffraction of single crystals, data were collected on a MacScienceDIPLabo Imaging Plate diffractometer, λ(Cu Kα) = 1.5418 Å. The structure was solved by direct methods and expanded using Fourier techniques. All calculations were performed with the crystallographic software package SHELX-97.

3: C$_{12}$H$_8$O$_4$, M_W = 216.18, monoclinic, *a* = 4.3980(2) Å, *b* = 12.2080(6) Å, *c* = 8.6590(5) Å, β = 102.870(4)°, *V* = 453.23(4) Å^3, D_{calcd} = 1.584 g/cm^3, *T* = 193 K, space group P2$_1$/c (#14), *Z* = 2, μ(Cu Kα) = 10.5 cm^{-1}, 4150 reflections measured and 747 unique (2θ_{max} = 146.9°, R_{int} = 0.024), which were used in all calculations. *R* = 0.062, R_w = 0.181.

4: C$_{12}$H$_8$O$_4$, M_W = 216.18, monoclinic, *a* = 4.8840(5) Å, *b* = 12.39640(7) Å, *c* = 15.3700(17) Å, β = 92.857(8)°, *V* = 447.14(9) Å^3, D_{calcd} = 1.606 g/cm^3, *T* = 193 K, space group P2$_1$/n (#14), *Z* = 2, μ(Cu Kα) = 10.29 cm^{-1}, 4324 reflections measured and 623 unique (2θ_{max} = 146.9°, R_{int} = 0.032), which were used in all calculations. *R* = 0.106, R_w = 0.311.

Supporting Information Available: The assignment of ^{1}H and ^{13}C NMR chemical shifts, including the spectra of new compounds (**2**, **4**, **6**, and **8**), crystallographic information format (CIF) files for **3** and **4**, and numerical data for ab initio calculations. This material is available free of charge via the Internet at http://pubs.acs.org.

JO802345F